Extrasynaptic glutamate release through cystine/glutamate antiporter contributes to ischemic damage

Federico N. Soria,[1] Alberto Pérez-Samartín,[1] Abraham Martin,[2] Kiran Babu Gona,[3] Jordi Llop,[3] Boguslaw Szczupak,[2] Juan Carlos Chara,[1] Carlos Matute,[1] and María Domercq[1]

[1]Centro de Investigaciones Biomédicas en Red (CIBERNED), Achucarro Basque Center for Neuroscience and Departamento de Neurociencias, Universidad del País Vasco (UPV/EHU), Leioa, Spain.

[2]Molecular Imaging Unit and [3]Radiochemistry Department, CIC biomaGUNE, San Sebastián, Spain.

During brain ischemia, an excessive release of glutamate triggers neuronal death through the overactivation of NMDA receptors (NMDARs); however, the underlying pathways that alter glutamate homeostasis and whether synaptic or extrasynaptic sites are responsible for excess glutamate remain controversial. Here, we monitored ischemia-gated currents in pyramidal cortical neurons in brain slices from rodents in response to oxygen and glucose deprivation (OGD) as a real-time glutamate sensor to identify the source of glutamate release and determined the extent of neuronal damage. Blockade of excitatory amino acid transporters or vesicular glutamate release did not inhibit ischemia-gated currents or neuronal damage after OGD. In contrast, pharmacological inhibition of the cystine/glutamate antiporter dramatically attenuated ischemia-gated currents and cell death after OGD. Compared with control animals, mice lacking a functional cystine/glutamate antiporter exhibited reduced anoxic depolarization and neuronal death in response to OGD. Furthermore, glutamate released by the cystine/glutamate antiporter activated extrasynaptic, but not synaptic, NMDARs, and blockade of extrasynaptic NMDARs reduced ischemia-gated currents and cell damage after OGD. Finally, PET imaging showed increased cystine/glutamate antiporter function in ischemic rats. Altogether, these data suggest that cystine/glutamate antiporter function is increased in ischemia, contributing to elevated extracellular glutamate concentration, overactivation of extrasynaptic NMDARs, and ischemic neuronal death.

Introduction

Brain ischemia is the fourth cause of death and the leading cause of long-term disability in industrialized countries (1). Relatively short periods of blood flow interruption in the brain can produce irreversible neuronal damage (2). Energy failure and oxygen deprivation that occur in ischemic episodes induce a loss of membrane potential in neurons and glia, a process known as anoxic depolarization (AD), which spreads across susceptible brain tissue as a self-propagating wave-like depolarization (3, 4) and can be initiated by factors that release K^+ and glutamate (4). Recordings from neurons in hippocampal and cerebellar slices have shown that this AD is associated with a large glutamate-evoked inward current, which can be blocked by a cocktail of agents blocking ionotropic glutamate receptors (5, 6). In particular, activation of NMDA receptors (NMDARs) plays a crucial role in neuronal cell death (7).

NMDAR-mediated signaling can be either beneficial or deleterious, and this dichotomous behavior has been proposed to be related to its localization within or outside the synapse (7, 8). Activation of NMDARs in synapses provides plasticity and cell survival signals, whereas extrasynaptic NMDARs trigger neurodegeneration (refs. 9–14; but see also refs. 15, 16). These opposing signals are transduced to and discriminated by the nucleus on the basis of the differential phosphorylation state of the Jacob protein messenger (13). However, most of these data have been obtained in vitro, and the role of synaptic or extrasynaptic NMDARs in ischemic neuronal damage has not been studied in a more intact preparation.

The functional dichotomy of NMDAR signaling would also depend on the location of the glutamate source. A major source of extrasynaptic glutamate is the cystine/glutamate antiporter (17), also known as system xc^-, a solute carrier identified as the main source of nonsynaptic glutamate in the brain (18–20). This transport system is a membrane-bound, Cl^--dependent, Na^+-independent antiporter that mediates the cellular uptake of cystine in exchange for glutamate at a 1:1 ratio (21–23). Structurally, it is a heterodimer composed of a heavy-chain subunit, 4F2hc, and a light-chain–specific subunit, xCT (24). System xc^- is an important source of cystine, which is intracellularly converted to cysteine, the rate-limiting substrate in glutathione synthesis (25). The high rate of oxygen consumption in the brain renders this antiporter vital to antioxidant defense (26), and its expression is rapidly upregulated in vitro under conditions of oxidative stress (27, 28). Nonetheless, the obligate exchange of

▶ Related Commentary: p. 3279

Conflict of interest: The authors have declared that no conflict of interest exists.
Submitted: July 9, 2013; **Accepted:** May 21, 2014.
Reference information: *J Clin Invest*. 2014;124(8):3645–3655. doi:10.1172/JCI71886.

glutamate, which is released into the extracellular space, could be deleterious to neuronal cells and other tissues that are susceptible to excitotoxic damage. Accordingly, the cystine/glutamate antiporter is implicated in glutamate-associated disorders such as glioma-derived epileptic seizures (29), oxidative glutamate toxicity (30), and excitotoxic oligodendroglial death (31).

Although ischemia is a disorder that occurs in an environment of oxidative stress and lack of nutrients, which are inducers of the cystine/glutamate antiporter (32), its contribution to glutamate homeostasis alteration and neuronal cell death after ischemia has not been explored before. Here, we analyze the contribution of different mechanisms of glutamate release, including the cystine/glutamate antiporter, and the role of synaptic versus extrasynaptic NMDARs in ischemia-gated currents and neuronal damage.

Results

Inhibition of glutamate transporters shortens the latency to AD and exacerbates neuronal damage in OGD. Na^+-dependent excitatory amino acid transporters (EAATs) could contribute to alter glutamate homeostasis during ischemic insults by 3 mechanisms: (a) decreased glutamate uptake, (b) reverse transport, and (c) heteroexchange. Severe chemical ischemic conditions decrease net glutamate uptake within 2 to 3 minutes (33), and at later stages, ischemia promotes reverse glutamate transport (5, 33). We therefore tested the effect of a broad-spectrum nonsubstrate antagonist of EAATs, DL-threo-β-benzyloxyaspartic acid (TBOA; 100 μM) on OGD-gated currents in pyramidal cells from acute cortical slices, and its effect on neuronal cell death in organotypic cortical slices. OGD activated a large inward current within 12 minutes (Figure 1, A and B), which corresponds to AD. This current was mainly mediated by glutamate receptors, since a cocktail of ionotropic glutamate receptor antagonists (100 μM AP5 plus 30 μM CNQX) applied concomitantly with OGD greatly reduced OGD-gated currents (Figure 1, A and B). Reduction of AD was not complete, suggesting that other channels, such as the acid-sensitive anion channel (34), the P2X7 receptor (35, 36), and pannexin 1 (37), also contribute to the OGD current.

Application of TBOA during OGD did not decrease the amplitude of the OGD-activated current (Figure 1, A and B). Furthermore, TBOA reduced the latency to onset of AD in 3 minutes (Figure 1B), as previously observed by others (38). This implies that in this paradigm, most transporters are still active and work in direct uptake mode at the beginning of ischemia, since its chronic blockade during OGD results in increased concentrations of glutamate and reduced latencies to AD. Indeed, we found that OGD-activated currents in the presence of TBOA were similarly blocked by glutamate receptor antagonists (Figure 1, A and B). EAATs reverse as a result of alterations in the transmembrane gradients once AD has been initiated (33). Thus, to ensure that we were blocking EAATs when they are mostly in reverse-uptake mode, we applied TBOA at the peak of the AD. Blockade of EAATs after the onset of AD still potentiated the amplitude of AD current (Figure 1C), suggesting that, despite the strongly reduced transmembrane sodium and potassium concentration gradients, EAAT still takes up glutamate during AD, and its blockade further enhances extracellular glutamate accumulation. Although these results do not rule out that OGD partially reduces glutamate uptake or that a minor population of EAATs could indeed be working in reverse-uptake mode, they strongly suggest that another source of glutamate contributes to the alteration of glutamate homeostasis in ischemia.

We also tested the effect of EAAT blockade in cell death using organotypic cortical slices (39). TBOA exacerbated cell death after OGD and reoxygenation, as assessed by lactic dehydrogenase (LDH) release assays (Figure 1D, and see also in Supplemental Figure 1 the effect of TBOA in normoxia; supplemental material available online with this article; doi:10.1172/JCI71886DS1). Parallel staining with propidium iodide revealed cell death in the cortex, which was proportional to the damage quantified by LDH release (Figure 1E). TBOA-mediated exacerbation in excitotoxic damage in hypoxia/ischemia has also been observed in cultured neurons (16) and organotypic cortical slices (40), confirming the primary physiological role of EAATs in the clearance of extracellular glutamate.

Inhibition of exocytosis has no effect on ischemia-gated currents or cell death. An increase in vesicular synaptic glutamate release and in miniature excitatory postsynaptic currents (mEPSCs) occurs at early phases of ischemia and before AD (33, 41, 42). We therefore tested whether vesicular release was contributing to the increase in AD currents in acute slices by using bafilomycin A1 (Baf A1; 1 μM), a vacuolar type H^+-ATPase inhibitor, to block neurotransmitter loading into synaptic vesicles. Baf A1 practically abolished the mEPSCs (Supplemental Figure 2), thus indicating an effective inhibition of spontaneous vesicular glutamate release. In contrast, we found that neither the latency nor the amplitude of the anoxic current was changed when Baf A1 was present at the onset of OGD (Figure 2, A and B). Accordingly, neuronal damage was not significantly different in Baf A1–treated (1 μM) or tetanus toxin–treated (TeTN-treated; 1 μg/ml) slices compared with OGD alone (Figure 2, C and D). These results suggest that vesicular release after OGD does not significantly contribute to AD currents and toxicity and are consistent with an extrasynaptic source of glutamate in ischemia.

Blockade of the cystine/glutamate exchanger reduces ischemia-gated currents and neuronal damage after OGD. The cystine/glutamate antiporter reportedly regulates extracellular glutamate concentration in physiological (20, 43) and pathological conditions (19, 29, 31). We next analyzed whether ischemia-induced glutamate release might be caused as a result of cystine exchange by system xc^-. To analyze the possible contribution of the cystine/glutamate antiporter to glutamate release during OGD, we applied S-4-carboxyphenylglycine (CPG; 250 μM) (Figure 3A), a nonsubstrate inhibitor of the antiporter (refs. 44, 45, and see also Supplemental Figure 3). We found that although CPG did not change latency to AD, it significantly reduced its amplitude (Figure 3, A and B). We further assessed the effect of CPG on extracellular direct-current (DC) field potentials (46) and showed that CPG significantly reduced the ΔV_o amplitude after OGD (Figure 3C). Because CPG is also a competitive inhibitor of group I metabotropic glutamate receptors ($mGluR_I$) (47), we also tested sulfasalazine (SAS; 250 μM), another nonsubstrate inhibitor of the cystine/glutamate antiporter (44, 45) with no affinity for glutamate receptors, and obtained a similar attenuation of the AD current (Figure 3, A and B). In contrast,

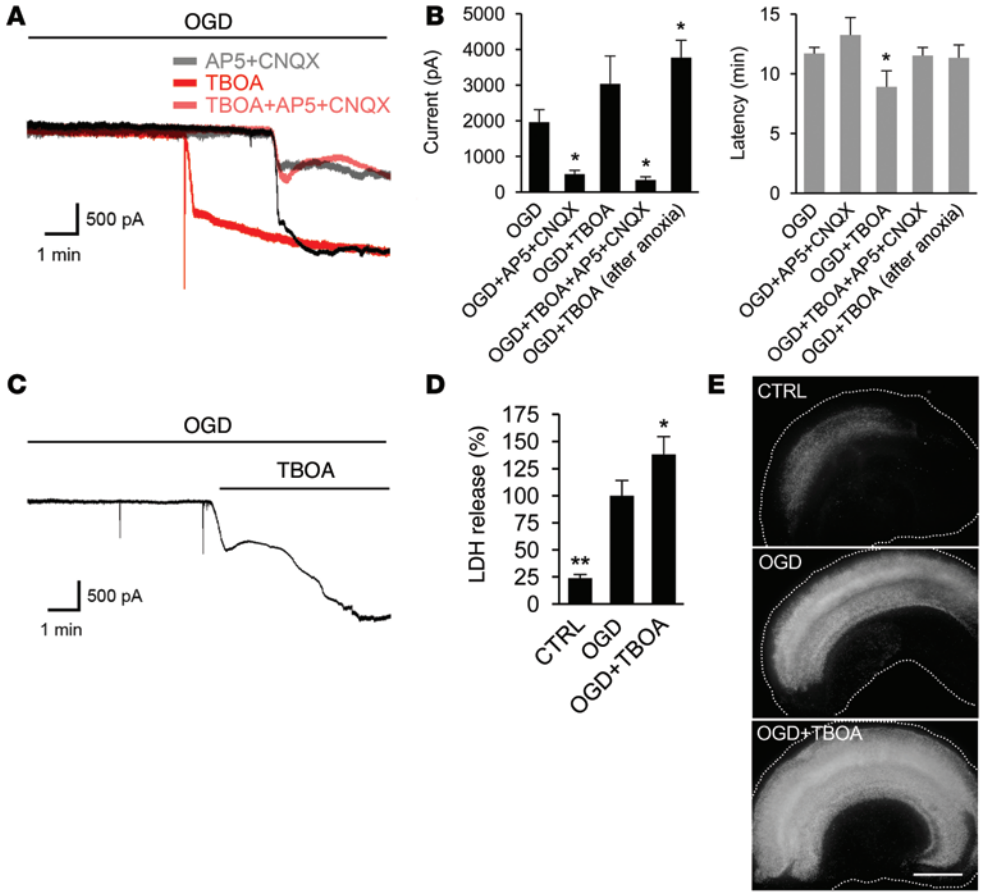

Figure 1. Blockade of EAATs during OGD contributes to extracellular glutamate accumulation in acute slices and organotypic cultures. (**A**) Voltage-clamp recording of cortical neurons at 30 mV in acute slices demonstrates activation of a large current after OGD (n = 32). Ionotropic glutamate receptor antagonists AP5 (100 μM) plus CNQX (30 μM) significantly inhibited the OGD-activated current (n = 9). Nonsubstrate broad-spectrum EAAT inhibitor DL-TBOA (100 μM) did not significantly change (but tended to increase) the amplitude of the OGD-induced current and shortened the onset of AD in cortical neurons (n = 12), an effect abolished when applied concomitantly with AP5 plus CNQX (n = 7). (**B**) Histograms showing the average amplitude (pA ± SEM) and latency (minutes ± SEM) of the OGD-induced current for each condition. Latency was significantly reduced in the presence of TBOA. *P < 0.05 versus OGD. (**C**) TBOA increased the OGD-activated current when applied after the onset of AD (n = 11). (**D**) Inhibition of EAATs exacerbated OGD-induced cell death in organotypic slices, as demonstrated by increased LDH release in cultures subjected to 45 minutes of OGD and 24 hours of reoxygenation in the presence or absence of TBOA (100 μM). Data are expressed as the mean ± SEM (n = 3–5). **P < 0.01 and *P < 0.05 versus OGD. (**E**) Representative fields demonstrate propidium iodide labeling in cortical layers of slices treated as in **D**. Scale bar: 1 mm.

AIDA (500 μM), a selective inhibitor of $mGluR_1$, did not affect the OGD-activated current (Figure 3, A and B), excluding any role of these receptors in the effect observed with CPG. Interestingly, we did not observe an increase in the amplitude of OGD currents in TBOA-treated slices in the presence of CPG (compare Figure 1, A and B with Figure 3, B and D), which suggests that blockade of glutamate uptake by EAATs does not increase glutamate extracellular levels when the source of glutamate, cystine/glutamate antiporter, is inhibited. These data are in accordance with data in normoxic conditions (48) and reinforce the important role played by the cystine/glutamate antiporter in glutamate homeostasis during ischemia. It should be stressed, however, that the latency to AD was still reduced when TBOA was present along with CPG (Figure 3B and see also Figure 1B).

Next, we investigated whether pharmacological inhibition of the cystine/glutamate antiporter reduced ischemic damage in cerebral cortex organotypic slices. Inhibition of system xc^- with CPG and SAS (250 μM) significantly reduced neuronal damage after OGD (Figure 3, E and F) in a way similar to the neuroprotection observed with NMDAR antagonist MK-801 (50 μM; Figure 3, E and F). In contrast, no inhibition of OGD-induced neuronal damage was detected with the $mGluR_1$ antagonist AIDA (500 μM; Figure 3, E and F). To further confirm the role played by the cystine/glutamate antiporter, we performed additional experiments in mutant mice lacking a functional system xc^- (*Slc7a11sut*). These mice (49) have a large spontaneous deletion from intron 11 to the adjacent *sut* region of the *Slc7a11* gene, leading to a truncated and nonfunctional xCT protein. As observed with the system xc^- inhibitors, *sut* mice showed a significant reduction in anoxic currents (Figure 4, A and B), DC extracellular potential shifts (Figure 4C), and neuronal damage after OGD (Figure 4, D and E). Altogether, these data suggest that the cystine/glutamate antiporter is a relevant source of glutamate release during ischemia and that its inhibition is neuroprotective against ischemic neuronal damage.

Cystine/glutamate antiporter activates extrasynaptic NMDARs in cortical neurons. Although the cystine/glutamate antiporter has been proposed as an important source of nonsynaptic glutamate (17, 19, 20), there is no direct link between glutamate release by this transport system and the activation of extrasynaptic glutamate receptors. Previous data showed that glutamate release by the cystine/glutamate antiporter evokes glutamate receptor–mediated inward currents in Purkinje cells upon acute exposure to cystine (50). Hence, we next analyzed whether glutamate release induced by acute cystine application could activate synaptic and/or extrasynaptic NMDARs. Cortical neurons were clamped at –30 mV to remove Mg^{2+} block from NMDARs, and cystine (1 mM) was applied concomitantly with glycine (10 μM). Cystine evoked an inward current in most cells, with a mean value 310 ± 53 pA, while glycine alone only induced small inward currents (Figure 5). Cystine-evoked currents

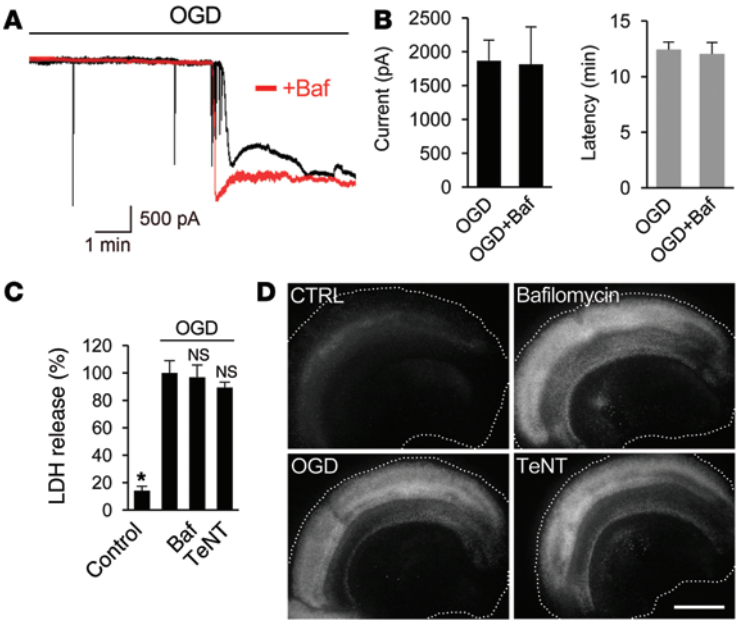

Figure 2. Inhibition of vesicular glutamate release does not change anoxic current or cell death in OGD. (**A**) OGD-activated currents (recorded at 30 mV) in the absence or presence of vesicular fusion inhibitor Baf A1 (μM). (**B**) Histograms show the average amplitude (pA ± SEM) and latency (minutes ± SEM) of the OGD-induced current for each condition. Baf did not change the amplitude or latency of the OGD-activated current (n = 7). (**C**) Cell death measured by LDH release in cultures subjected to 45 minutes of OGD and 24 hours of reperfusion in the presence or absence of the exocytosis inhibitors Baf (1 μM) and TeNT (1 μg/ml). Data are expressed as the mean ± SEM (n = 3–5). *P < 0.001 versus OGD. (**D**) Representative fields showing propidium iodide labeling of organotypic slices treated as in **C**. Scale bar: 1 mm.

were completely abolished in the presence of the NMDA antagonist AP5 (50 μM; Figure 5). To exclude a direct action of cystine (plus glycine, 10 μM) on NMDARs, we applied cystine in the presence of the cystine/glutamate antiporter blocker CPG (250 μM). Cystine-evoked currents were significantly inhibited by CPG (Figure 5), suggesting that cystine evokes glutamate release and indirectly activates NMDARs.

According to their localization in the cell membrane, NMDARs differ in their subunit composition. Thus, synaptic NMDARs are enriched in NR2A subunits, while NR2B subunits are located mainly in extrasynaptic NMDARs (8, 51–53). This feature allows for pharmacological blockade of either subtype by using subunit-specific antagonists. RO-256981 (1 μM), an NR2B antagonist (54), almost totally blocked cystine-evoked inward currents (Figure 5). In contrast, NVP-AAM077 (250 nM), which preferentially inhibits NR2A-containing receptors (55), did not change the amplitude of cystine-evoked inward currents (Figure 5). These data suggest that glutamate release in exchange with cystine activates preferentially extrasynaptic NMDARs.

Antagonists of extrasynaptic, but not of synaptic, NMDARs attenuate ischemia-gated currents and cell death after OGD. If the cystine/glutamate exchanger regulates extrasynaptic glutamate levels as previously demonstrated (Figure 5), then glutamate released during OGD would favor the activation of extrasynaptic NMDARs over synaptic ones. Hence, we analyzed the contribution of synaptic and extrasynaptic NMDARs to ischemic inward currents and neuronal damage. We observed a significant reduction in OGD-activated currents in the presence of ifenprodil (3 μM; Figure 6, A and C), a known NR2B antagonist (56). RO-256981 (1 μM), a more potent antagonist of NR2B (54), produced a 3-fold reduction in the amplitude of the OGD-activated current (Figure 6, A and C). In contrast, the NR2A antagonists NVP-AAM077 (250 nM) and TCN-201 (10 μM) (55, 57) did not change the amplitude of OGD-activated currents (Figure 6, B and C). Finally, memantine, which at 10 μM preferentially blocks extrasynaptic receptors without interfering with synaptic activity (58, 59), also reduced the anoxic current (Figure 6, A and C). None of the antagonists, independently of their subunit specificity, altered the latency to the anoxic current (Figure 6C). These results suggest that NR2B-containing receptors play a role in AD in ischemia.

Finally, we checked the contribution of synaptic and extrasynaptic NMDARs to neuronal damage after OGD in organotypic cortical cultures. The NR2A antagonists NVP-AAM077 (55, 60) and TCN-201 (57) did not reduce cell death significantly (Figure 6, D and E). It should be noted, however, that high concentrations of glycine in culture medium during reperfusion may reduce TCN-201 effectiveness (57). In contrast, memantine (10 μM) and RO-256981 (1 μM) produced a massive reduction in OGD-induced cell death (Figure 6, D and E). Neuroprotection with memantine was similar to that obtained with the NMDAR antagonist MK801 (50 μM; Figure 6, D and E). Altogether, these data indicate that activation of extrasynaptic NMDARs contributes substantially to excitotoxic death during OGD in organotypic cortical cultures and suggest that these receptors are likely activated by extrasynaptic tonic release of glutamate from the cystine/glutamate antiporter.

xCT expression and function are increased after ischemia in vitro and in vivo. The excessive release of glutamate that causes neuronal death during brain ischemia takes place in an environment of oxidative stress (61), a condition that favors an increase in the expression and function of the cystine/glutamate antiporter (23, 32). Therefore, we next analyzed the expression levels of the catalytic subunit of the cystine/glutamate antiporter xCT in cortical neuron cultures exposed to chemical ischemia in vitro, ischemic conditions that induced massive cell death (70.65 ± 7.43%) and reproduced metabolic failure in the ischemic core. Real-time quantitative PCR (qPCR) analysis demonstrated that *xCT* mRNA was significantly more abundant (80%) in neurons after 1 hour of chemical ischemia (Figure 7A). To examine xCT levels by immunoblotting, total protein was extracted 4 hours after chemical ischemia to allow the translational machinery to produce xCT.

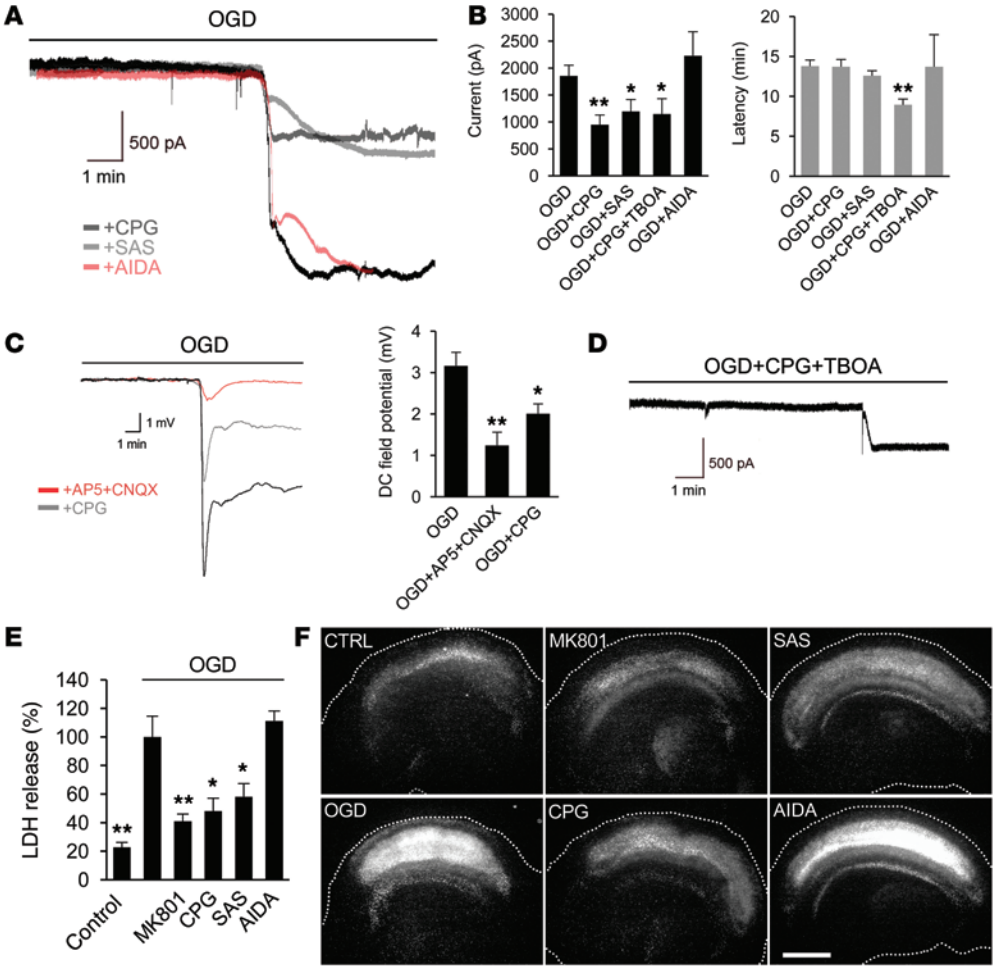

Figure 3. Inhibition of the cystine/glutamate antiporter reduces the OGD-induced current, DC depolarization, and cell death. (**A**) Voltage-clamp recording of OGD-activated currents in the absence or presence of system xc^- inhibitors CPG (250 μM; $n = 12$) and SAS (250 μM; $n = 10$). Both treatments significantly inhibited the OGD-activated current ($n = 25$). The $mGluR_1$ inhibitor AIDA (500 μM; $n = 6$) had no effect on anoxic current amplitude or on latency. (**B**) Histograms show the average OGD-induced current amplitude (pA ± SEM) and latency (minutes ± SEM) for each condition. $^{**}P < 0.01$ and $^{*}P < 0.05$ versus OGD. (**C**) AD was recorded as a negative DC field voltage shift in acute cortical slices subjected to OGD in the absence or presence of the ionotropic glutamate receptor antagonists AP5 and CNQX or of the cystine/glutamate antiporter inhibitor CPG. Histogram shows the average DC potential shift (mV ± SEM) for each condition. $^{**}P < 0.01$ and $^{*}P < 0.05$ versus OGD. (**D**) TBOA applied concomitantly with CPG did not enhance the CPG-induced decrease of the OGD current amplitude, but reduced the latency to AD ($n = 6$). (**E**) Cell death measured by LDH release in cultures subjected to 45 minutes of OGD applying system xc^- inhibitors CPG (250 μM; $n = 5$) and SAS (250 μM; $n = 5$), NMDAR antagonist MK-801 (50 μM, $n = 5$), and $mGluR_1$ antagonist AIDA (500 μM; $n = 3$). LDH was measured after 24 hours of reoxygenation, and data are expressed as the mean ± SEM. $^{*}P < 0.05$ and $^{**}P < 0.01$ versus OGD. (**F**) Representative fields demonstrate propidium iodide labeling of organotypic slices treated as in **E**. Scale bar: 1 mm.

Western blot analysis revealed a 2-fold increase in xCT protein in neurons exposed to chemical ischemia (Figure 7B). This increase in xCT levels at 4 hours of reoxygenation is consistent with the fact that reactive oxygen species are generated not only during ischemia, but also during the reoxygenation period as a result of the activation of NADP(H) oxidase (61). To confirm these findings, we next examined the cystine transport activity of system xc^- by measuring [^{14}C] L-cystine uptake in neurons exposed to 1 hour of chemical ischemia plus 4 hours of reoxygenation. Specific Cl^--dependent cystine uptake by system xc^- was defined as the differential cystine uptake in the presence and absence of Cl^-. Specificity was further assessed using the system xc^- competitive inhibitor aminoadipic acid (AAA; 250 μM), which significantly blocked [^{14}C] L-cystine uptake. In accordance with Western blot data, cystine uptake by the antiporter was increased in neurons subjected to chemical ischemia (Figure 7C). Altogether, these data reveal an increase in neuronal xCT expression and function after in vitro ischemia.

Next we analyzed the function of cystine/glutamate antiporter short times (5 minutes and 5 hours) after inducing transient focal ischemia via middle cerebral artery occlusion (MCAO) in rats. In order to measure xCT function in vivo, we took advantage of the recently developed radioligand (4S)-4-(3-[18F]fluoropropyl)-L-glutamate (^{18}[F]FSPG) to image xCT transporter activity by PET (62). As previously described (63), the brain showed low ^{18}[F]FSPG uptake. However, we observed tracer accumulation as a result of higher activity of the cystine/glutamate antiporter in the ipsilateral hemisphere immediately after initiation of reperfusion (PET imaging could not be performed during MCAO), and this accumulation peaked at the striatum at 5 hours (Figure 7, D and E). This is in agreement with the fact that MCAO induces early striatal infarction (4 hours) but delayed necrosis in the cortex (>12 hours) (64). Altogether, these data indicate that the cystine/glutamate antiporter increases its expression and activity following ischemia and further support the relevance of this antiporter in glutamate homeostasis alteration in stroke.

Discussion

While glutamate-induced excitotoxicity is widely accepted as a critical event that leads to neuronal death during ischemia, several other questions have yet to be answered. For instance, the mechanisms behind the alteration in glutamate homeostasis and the balance between the release and clearance of glutamate in ischemia are not yet completely understood, and the location of the gluta-

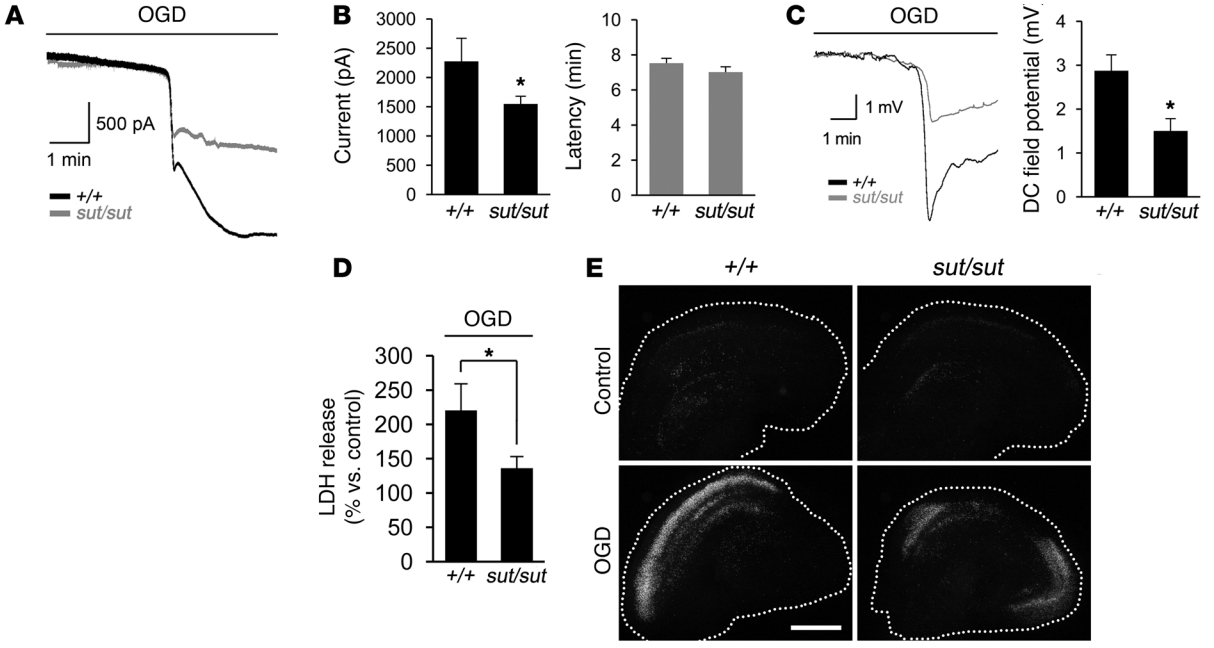

Figure 4. AD and OGD-induced cell death are reduced in *Slc7a11sut* mice, which lack a functional cystine/glutamate antiporter. (**A**) Voltage-clamp recording of OGD-activated currents in mouse acute slices. The anoxic current amplitude was reduced in the xCT-deficient (*sut/sut*; $n = 13$) mice when compared with that in wild-type mice ($^{+/+}$; $n = 14$). However, the latency to AD was unchanged. (**B**) Histograms show the average amplitude (pA ± SEM) and latency (minutes ± SEM) of the OGD-induced current for each genotype. $^*P < 0.05$. (**C**) Simultaneous extracellular DC field potential recording in acute slices from wild-type and *sut/sut* mice subjected to OGD. Histogram shows the average DC field potential (mV ± SEM) for each genotype. $^*P < 0.05$. (**D**) Cell death measured by LDH release in organotypic cultures from wild-type and *sut/sut* mice exposed to 45 minutes of OGD and 24 hours of reoxygenation. Data are expressed as the mean ± SEM ($n = 3$). (**E**) Representative fields demonstrate propidium iodide labeling of organotypic slices treated as in **D**. Scale bar: 1 mm.

mate receptors that trigger the death signal in ischemia is still controversial. The data reported here provide evidence that glutamate release by the cystine/glutamate antiporter contributes to ischemia-induced anoxic currents and neuronal damage. Electrophysiology data suggest that glutamate release by system xc^- activates mainly extrasynaptic NMDARs. Accordingly, blocking extrasynaptic, but not synaptic, NMDARs reduces ischemia-induced currents and cell damage. Finally, in vivo PET imaging indicated that system xc^- function was robustly increased during ischemia and reperfusion, suggesting a further contribution to glutamate release and cell death. To our knowledge, this is the first report of the contribution of the cystine/glutamate antiporter to glutamate homeostasis alteration and subsequent cell death in ischemia.

Activation of the cell death program in neurons appears to be linked to the overstimulation of extrasynaptic NMDARs (8, 13). Our data suggest that extrasynaptic NR2B-containing receptors are the main contributors to anoxic currents and neuronal damage in OGD. Accordingly, previous data showed that cerebral ischemia recruits death-associated protein kinase 1 (DAPK1) to the NR2B complex at extrasynaptic sites, and this interaction functions as a central mediator of stroke damage (12). In contrast, preblocking synaptic NMDARs with MK801 has been reported to protect cultured hippocampal neurons against hypoxic damage (16). The role of synaptic and extrasynaptic receptors in neuronal cell death is currently a matter of intense debate (7–16). It is known that NR2B subunits segregate outside the synapses (51, 65), whereas NR2A subunits are confined to the postsynaptic membrane (53). The different availability of endogenous coagonists D-serine and glycine, which show activation selectivity for NR2A and NR2B, respectively, also contributes to segregate NMDARs at specific locations (15). However, it is possible that such segregation is an oversimplification (66), and additional tools to specifically block each receptor will be necessary in the future.

The role played by synaptic and extrasynaptic NMDARs in neuronal cell death in neurological diseases would depend on the source of glutamate. Glutamate levels outside the synaptic cleft are maintained by nonvesicular release through system xc^- (18–20), and glutamate released by the cystine/glutamate antiporter is sufficient to activate glutamate receptors (20, 29, 50). We observed that glutamate release by system xc^- preferentially activated extrasynaptic NR2B receptors. Moreover, nonsubstrate inhibitors of system xc^- significantly attenuated the anoxic currents and ischemic damage, results confirmed in mutant *sut* mice, in which xCT is nonfunctional ($P < 0.05$). This strongly suggests a role for the cystine/glutamate antiporter as a source of glutamate in ischemia. We thus propose that an important source of glutamate in this pathology is extrasynaptic, a finding further supported by our observations that vesicular inhibitor Baf A1 did not affect ischemic currents or neuronal damage.

It should be noted that latency to AD was still reduced when CPG was applied concomitantly with TBOA (therefore, glutamate clearance was inhibited), suggesting that another source of glutamate contributes to altering glutamate homeostasis. Severe ischemic conditions may induce the reversion of glutamate transporters (5). However, glial glutamate transporters do not readily reverse and remain functional during ischemia (38, 67). In accordance,

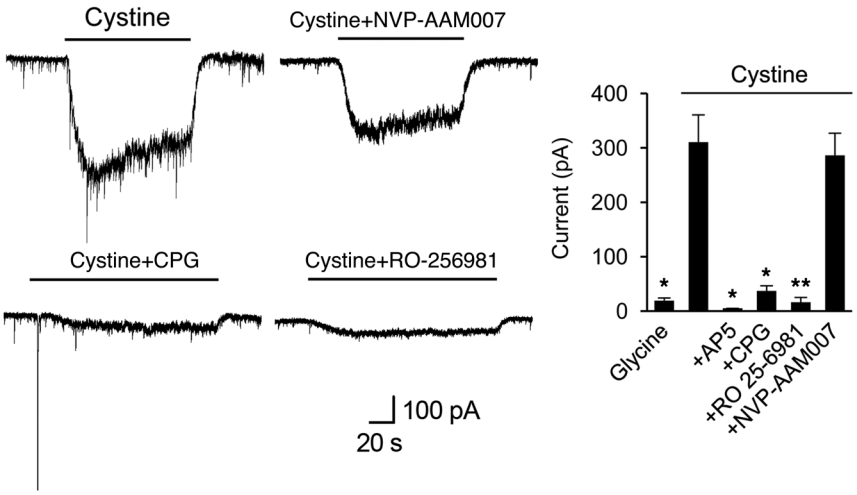

Figure 5. Cystine-evoked (1 mM) inward currents in pyramidal cortical neurons (n = 21). Currents were blocked in the presence of CPG (50 μM; *n* = 5), the NMDAR antagonist AP5 (50 μM; *n* = 5), and the NR2B antagonist RO-256981 (1 μM; *n* = 6), but not in the presence of the NR2A antagonist NVP-AAM077 (250 nM; *n* = 6). $^{*}P < 0.05$; $^{**}P < 0.01$.

we found that blocking glutamate transporters shortened latency to AD, amplified the anoxic current at the peak of AD, and, consequently, increased neuronal damage (see also refs. 16, 40). These data do not exclude the possibility that a small proportion of glutamate transporters (i.e., neuronal EAAT3) function in reverse mode, though inhibition of EAATs mostly in astrocytes leads to glutamate accumulation. It is worth noting that the latency to AD was significantly increased in *Eaac1*$^{-/-}$ (38), but not in *Eaat2*$^{-/-}$, mice (67).

Another possible source of glutamate is vesicular release. An increase in mEPSCs has been described previously at early phases of ischemia, before AD (33, 38, 41). The increase in mEPSC frequency was Ca^{2+} independent and caused by ischemia-induced actin filament depolymerization (41). However, the increased spontaneous vesicular transmitter release caused by energy depletion only leads to extracellular glutamate accumulation when glial glutamate uptake is blocked (33). Accordingly, we did not detect any change in anoxic currents or damage in the presence of Baf A1 or TeTN. In conclusion, this work does not challenge the current notion that exocytosis or EAATs are key contributors to the release of ischemic glutamate, but suggests that other sources of neurotransmitters (and in particular the cystine/glutamate antiporter) are contributing to the process.

Several reports of glutamate release in pathological conditions by this antiporter have been published recently, and a link between glutamate release by system xc^- and some CNS diseases has been established. Thus, xCT silencing diminished glutamate secretion from gliomas and alleviated neurodegeneration (68) or epileptic seizures (29). Similarly, inhibition of cystine/glutamate antiporter–mediated glutamate release secondary to either microglial activation (31) or Parkinson-inducing toxin 6-hydroxydopamine (19) prevented glial and neuronal damage. On the other hand, expression of the catalytic subunit xCT is augmented in processes that involve oxidative stress such as inflammation (69), viral infection (70), and tumor proliferation (71). We also detected an increase in xCT expression and function in primary cortical neurons. Furthermore, we have used for the first time a tracer specific for the system xc^- in brain in a live animal to monitor cystine/glutamate antiporter activity during ischemia and reperfusion. We found that ischemia induced a rapid increase in system xc^- activity in vivo. This augmented function after ischemia would contribute to further alter glutamate homeostasis during reperfusion.

A better understanding of the alterations of glutamate homeostasis in ischemia is a key challenge for the field. Protecting neurons from ischemic excitotoxic damage by inhibiting ionotropic glutamate receptors has been a useful strategy that has rendered promising results both in vitro and in vivo. However, clinical trials did not provide satisfactory results, because the use of glutamate receptor antagonists has many secondary effects that are detrimental to patients. Therefore, blocking the source of glutamate rather than the site of action may be a relevant therapeutic intervention for the prevention of ischemic brain injury.

Methods

Reagents and chemicals. Calcein-AM and all cell culture supplies were purchased from Invitrogen. The cytotoxicity assay for the quantification of LDH release was acquired from Roche. L-cystine, NVP-AAM077, propidium iodide, SAS, iodoacetate, and TeNT were obtained from Sigma-Aldrich. Baf A1, bicuculine, D-AP5, CNQX, ifenprodil, MK801, memantine, RO 25-6981, CPG, DL-TBOA, AIDA, and TCN-201 were purchased from Tocris.

Mice and genotyping. Mutant *Slc7a11sut* mice lacking the cystine/glutamate antiporter (49) and wild-type C3H/HeSnJ mice were purchased from The Jackson Laboratory. We used littermates for all experiments. For PCR genotyping, 2 sets of primers were designed: Rv-E12 (5′-CAAGGCCTCAAGCCCCTG-3′), which matches to exon 12 of the *Slc7a11* gene only in $^{+/+}$ mice (this region is deleted in *sut* mice), and Rv-E12′ (5′-ATTTGACCACAATCTTTGAGACCA-3′), which hybridizes an alternative exon 12 (E-12′) located within amplification range only in *sut* mice. The forward primer used in both cases was Fw-E11 (5′-TGAAACATGGAAACCGAAATCAC-3′), which hybridizes to exon 11 of *Slc7a11*.

Electrophysiology. Cortical slices (250-μm) from P18 to P25 Sprague-Dawley rats (except for NMDA antagonist experiments, in which P25 to P30 rats were used) and from P25 to P30 C3H/HeSnJ mice were prepared in artificial cerebrospinal fluid (aCSF; pH 7.4) that contained 126 mM NaCl, 24 mM $NaHCO_3$, 1 mM NaH_2PO_4, 2.5 mM KCl, 2.5 mM $CaCl_2$, 2 mM $MgCl_2$, and 10 mM D-glucose constantly bubbled with 95% O_2 and 5% CO_2. Slices were allowed to recover for at least 1 hour and were then transferred to a 37°C chamber with continuous flow (1 ml/minute) with aCSF plus bicuculline (100 μM) to block GABA receptors and cystine (10 μM). Pyramidal cells of layer V of the cortex

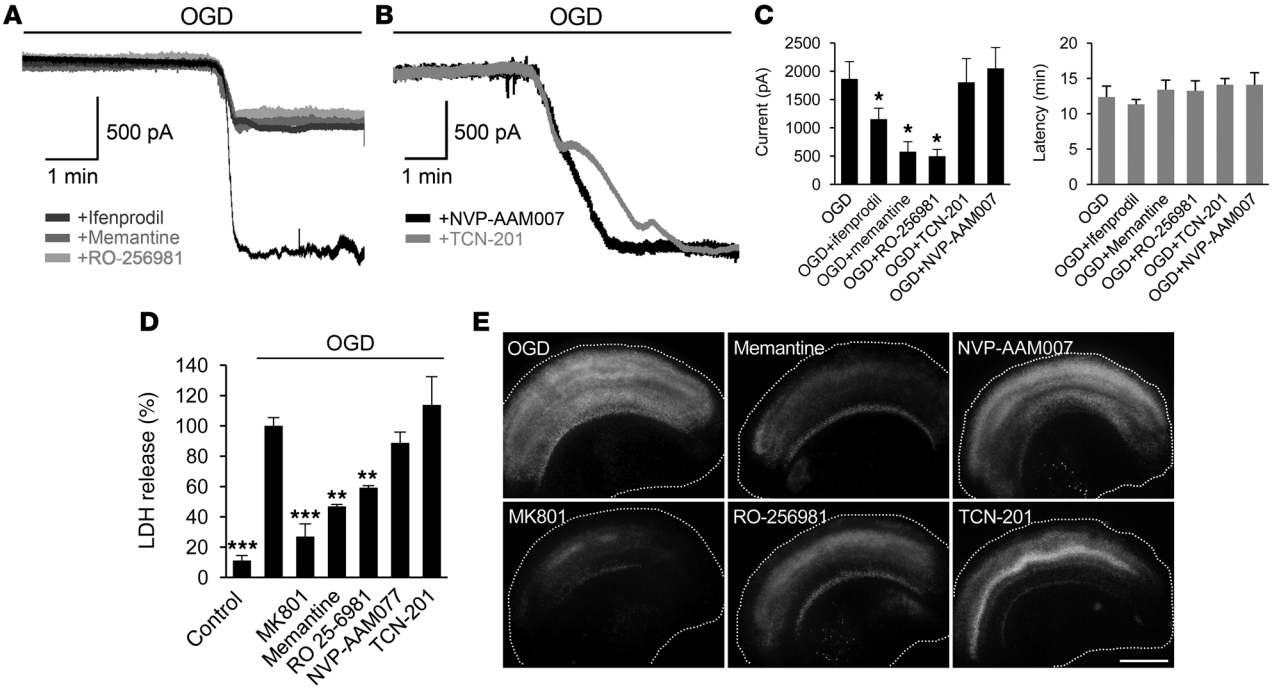

Figure 6. Blockade of extrasynaptic NMDARs attenuates OGD-induced currents and cell death. (**A** and **B**) Representative voltage-clamped recordings of cortical neurons at 30 mV in acute slices. OGD-activated currents were attenuated by the NR2B antagonists ifenprodil (3 μM; $n = 9$), memantine (10 μM; $n = 11$), and RO-256981 (1 μM; $n = 7$). NR2A antagonists TCN-201 (10 μM; $n = 6$) and NVP-AAM077 (250 nM; $n = 11$) failed to reduce OGD-gated currents. (**C**) Histograms showing the average amplitude (pA ± SEM) and latency (minutes ± SEM) of OGD-induced currents for each condition. $^*P < 0.05$ versus OGD. (**D**) Cell death measured by LDH release in organotypic cultures subjected to 45 minutes of OGD plus 24 hours of reoxygenation in the presence of the NR2B antagonists memantine (10 μM; $n = 4$) and RO-256981 (1 μM; $n = 3$) or of the NR2A antagonists TCN-201 (10 μM; $n = 3$) and NVP-AAM077 (250 nM; $n = 4$). MK801 (50 μM; $n = 5$) was also used to corroborate NMDA-mediated excitotoxicity. Data are expressed as the mean ± SEM. $^{**}P < 0.01$ and $^{***}P < 0.001$ versus OGD. (**E**) Representative fields demonstrate propidium iodide labeling of organotypic slices treated as in **D**. Scale bar: 1 mm.

were identified visually using infrared differential interference contrast (DIC) microscopy (Leica DM LFSA). Voltage-clamp recording pipettes (4–6 MΩ) were filled with a solution containing 135 mM CsCl, 4 mM NaCl, 0.7 mM $CaCl_2$, 10 mM BAPTA, 10 mM HEPES, 4 mM Mg-ATP, and 0.5 mM Na_2-GTP (pH 7.2). Access resistance and holding current were monitored throughout the experiment. To simulate ischemia, glucose was replaced with 10 mM sucrose, and 95% O_2/5% CO_2 was replaced with 95% N_2/5% CO_2. Cells were held at –30 mV to facilitate the sensing of ischemia-evoked currents through NMDARs. All antagonists were applied concomitantly with ischemia stimulation. For cystine puffs, a microperfusion manifold (World Precision Instruments) containing cystine (1 mM) plus glycine (10 μM) diluted with bathing solution was connected to an air-pressured system and placed into layer V of the cortex at a distance of 200 μm from the cell soma. Simultaneously with voltage-clamp recording, AD was recorded as negative extracellular DC potential shift (ΔV_o) induced by OGD. The DC potential is an extracellular recording that is considered to provide an index of the polarization of cells surrounding the tip of the glass electrode (2.5–7.5 MΩ) filled with 2 M NaCl (see ref. 72). For mEPSC recordings, refer to Supplemental Methods.

Organotypic slice cultures. Cultures were prepared from coronal cerebral sections (400-μm) of brains from 7-day-old Sprague-Dawley rat pups using the method described by Plenz and Kitai (73) with minor modifications (74). Cortex was sliced using a McIllwain tissue chopper (Mickle Laboratory Engineering Co.). Slices containing cortex and striatum (but not hippocampus) were selected under a microscope and dissected to eliminate the corpus callosum. Slices were plated onto Millicell CM culture inserts (Millipore) and maintained in 50% neurobasal-B27, 25% inactivated horse serum, 25% HBSS (all media from Invitrogen), 5.5 mM glucose, 2 mM L-glutamine, and 1X antibiotic-antimycotic (100 U/ml penicillin, 100 μg/ml streptomycin, and 0.25 μg/ml amphotericin B; Life Technologies) at 37°C and 5% CO_2. Slices were used after 12 to 14 days in vitro.

OGD (45 minutes) was achieved by incubating slices in an anaerobic chamber, in which O_2 was replaced with N_2 and external glucose (10 mM) with sucrose in an extracellular solution containing 130 mM NaCl, 5.4 mM KCl, 1.8 mM $CaCl_2$, 26 mM $NaHCO_3$, 0.8 mM $MgCl_2$, 1.18 mM NaH_2PO_4, and 10 μM L-cystine (pH 7.4). Organotypic cortical slices were washed with this solution (minus glucose) for 10 minutes prior to OGD to deplete the remaining glucose from extracellular spaces. After 45 minutes of OGD, extracellular solution was replaced with medium and O_2 supply restored. Antagonists were present during the preincubation (10 minutes), OGD (45 minutes), and reoxygenation (24 hours) periods. Cell death was determined 24 hours after OGD by measuring the release of LDH into the medium, using a colorimetric assay (Cytotoxicity Detection Kit; Roche Diagnostics) according to the manufacturer's instructions. To evaluate the damaged region within the slice, cultures were labeled with propidium iodide, the staining for which correlates with LDH release in models of excitotoxicity (75) and hypoxia (76). Briefly, after collecting media for the LDH assay, slices were incubated in propidium iodide–containing medium (10 μM) for 1 hour at 37°C. Slices were washed 3 times with culture medium and photographed using a Nikon AZ100 fluorescence microscope.

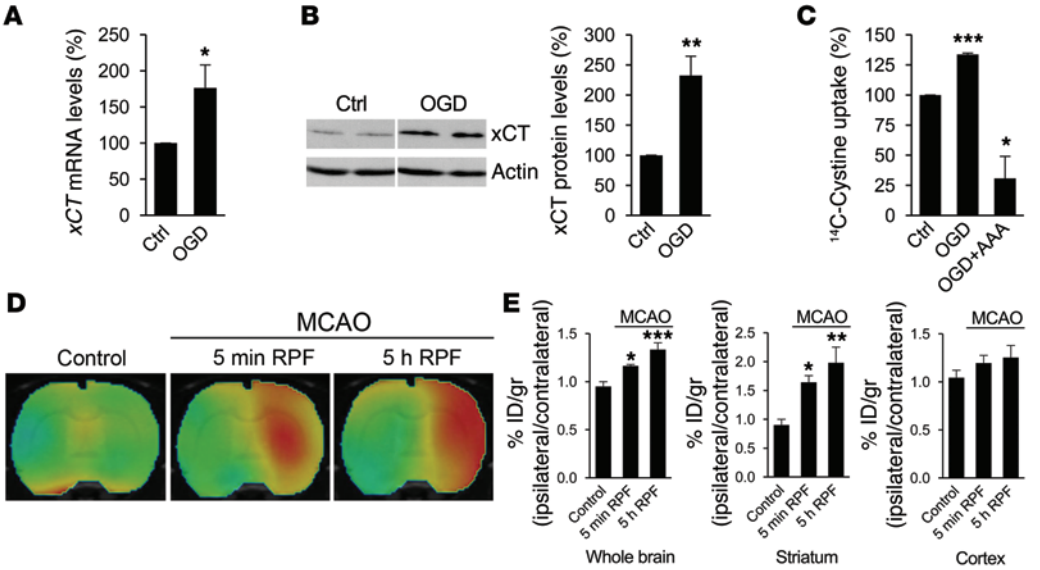

Figure 7. Cystine/glutamate antiporter expression and function are increased in cortical neurons in vitro after chemical ischemia and in vivo after transient focal ischemia. (**A**) *xCT* mRNA levels in neurons exposed to chemical ischemia (1 hour), as measured by qPCR. Data are expressed as the mean ± SEM ($n = 4$). (**B**) xCT protein levels after chemical ischemia (1 hour) plus a 4-hour reoxygenation in cortical neurons. Data were normalized to actin and are expressed as the mean ± SEM ($n = 4$). Control and OGD lanes were run on the same gel but were noncontiguous. Full, uncut gels are shown in the Supplemental Material. (**C**) Cl^--dependent [^{14}C] L-cystine uptake by neurons after 1 hour of chemical ischemia plus 4 hours of reoxygenation. Note that cystine/glutamate antagonist AAA (250 μM) almost completely inhibited uptake. Data were normalized to protein concentration and are expressed as the mean ± SEM ($n = 3$). (**D**) ^{18}[F]FSPG uptake study by PET imaging in control rats and after MCAO ($n = 5$ per group). Representative images of control rats and images at 5 minutes and at 5 hours of reperfusion (RPF) following MCAO. (**E**) Histogram shows ^{18}[F]FSPG signal expressed as the percentage of injected dose per gram (% ID/g) and normalized to the contralateral hemisphere in the total infarct area or in the volumes of interest (VOIs) defined in the striatum and cortex at 5 minutes or at 5 hours after reperfusion. Data are expressed as the mean ± SEM ($n = 5$). $^*P < 0.05$, $^{**}P < 0.01$, and $^{***}P < 0.001$ versus control.

Primary cortical neuron cultures. Primary neurons were obtained from the cortical lobes of E18 Sprague-Dawley rat embryos (77). Cells were resuspended in B27-supplemented neurobasal medium (Life Technologies) plus 10% FBS and then seeded onto poly-l-ornithine–coated glass coverslips at a density of 1.5×10^5 cells/cm^2. The medium was replaced with serum-free, B27-supplemented neurobasal medium 24 hours later. Cultures were essentially free of astrocytes and microglia and were maintained at 37°C and 5% CO_2. Cultures were used after 10 days in vitro. See Supplemental Methods for xCT expression and function assays after in vitro ischemia and glutamine synthetase assay using primary cortical neurons.

Transient focal ischemia. Transient focal ischemia was produced by a 2-hour intraluminal occlusion of the MCA followed by reperfusion in adult (10-week-old) male Sprague-Dawley rats obtained from Janvier (300 g body weight; $n = 10$), as described elsewhere (78). Briefly, rats were anesthetized with 4% isoflurane for 15 to 20 minutes in 100% O_2, and a 2.6-cm length of 4-0 monofilament nylon suture was introduced into the right external carotid artery up to the level where the MCA branches out, and animals were sutured and placed in their cages with ad libitum access to food and water. After 2 hours, the animals were reanesthetized, and the filament was removed to allow reperfusion and PET image acquisition. Animals were studied at 5 minutes ($n = 5$) and at 5 hours ($n = 5$) following the ischemic episode. See Supplemental Methods for details about the PET assay and radiosynthesis.

Statistics. Data are presented as the mean ± SEM (unless otherwise indicated) from at least 3 independent experiments, in which all conditions were assayed at least in triplicate. Comparisons between 2 groups were analyzed using an unpaired, 2-tailed Student's t test. Comparisons among multiple groups were analyzed by 1-way ANOVA followed by Bonferroni's multiple comparison tests for post hoc analysis. Statistical significance was considered at $P < 0.05$.

Study approval. Organotypic cultures, primary cultures, and electrophysiology protocols using rats and wild-type and *Slc7a11sut* mice were approved by the Comité de Ética y Bienestar Animal (Animal Ethics and Welfare Committee) of the UPV/EHU. MCAO and PET studies were approved by the animal ethics committee of CIC biomaGUNE and by local authorities and were conducted in accordance with the directives of the European Union on animal ethics and welfare.

Acknowledgments

The authors would like to thank to H. Gómez, S. Marcos, and S. Martín for technical assistance with cultures and electrophysiology studies; V. Gómez-Vallejo, M. González, and A. Leukona for technical support with radiosynthesis; and A. Cano, A. Arrieta, and M. Errasti for technical assistance in the PET studies. This work was supported by the Instituto de Salud Carlos III (fellowship to F.N. Soria); the Fundación Koplowitz; the Spanish Ministry of Education and Science (SAF2010-21547); the Basque Government; the UPV/EHU; and the CIBERNED.

Address correspondence to: Carlos Matute or Maria Domercq, Dpto. Neurociencias, Universidad del País Vasco, E-48940 Leioa, Spain. Phone: 3494.6013244; E-mail: carlos.matute@ehu.es (C. Matute). Phone: 3494.6015681; E-mail: maria.domercq@ehu.es (M. Domercq).

1. Burke JF, Lisabeth LD, Brown DL, Reeves MJ, Morgenstern LB. Determining stroke's rank as a cause of death using multicause mortality data. *Stroke*. 2012;43(8):2207–2211.
2. Lipton P. Ischemic cell death in brain neurons. *Physiol Rev*. 1999;79(4):1431–1568.
3. Dirnagl U, Iadecola C, Moskowitz MA. Pathobiology of ischaemic stroke: an integrated view. *Trends Neurosci*. 1999;22(9):391–397.
4. Somjen GG. Mechanisms of spreading depression and hypoxic spreading depression-like depolarization. *Physiol Rev*. 2001;81(3):1065–1096.
5. Rossi DJ, Oshima T, Attwell D. Glutamate release in severe brain ischaemia is mainly by reversed uptake. *Nature*. 2000;403(6767):316–321.
6. Hamann M, Rossi DJ, Mohr C, Andrade AL, Attwell D. The electrical response of cerebellar Purkinje neurons to simulated ischaemia. *Brain*. 2005;128(pt 10):2408–2420.
7. Tymianski M. Emerging mechanisms of disrupted cellular signaling in brain ischemia. *Nat Neurosci*. 2011;14(11):1369–1373.
8. Hardingham GE, Bading H. Synaptic versus extrasynaptic NMDA receptor signalling: implications for neurodegenerative disorders. *Nat Rev Neurosci*. 2010;11(10):682–696.
9. Hardingham GE, Fukunaga Y, Bading H. Extrasynaptic NMDARs oppose synaptic NMDARs by triggering CREB shut-off and cell death pathways. *Nat Neurosci*. 2002;5(5):405–414.
10. Zhang SJ, et al. A signaling cascade of nuclear calcium-CREB-ATF3 activated by synaptic NMDA receptors defines a gene repression module that protects against extrasynaptic NMDA receptor-induced neuronal cell death and ischemic brain damage. *J Neurosci*. 2011;31(13):4978–4990.
11. Zhang SJ, et al. Decoding NMDA receptor signaling: identification of genomic programs specifying neuronal survival and death. *Neuron*. 2007;53(4):549–562.
12. Tu W, et al. DAPK1 interaction with NMDA receptor NR2B subunits mediates brain damage in stroke. *Cell*. 2010;140(2):222–234.
13. Karpova A, et al. Encoding and transducing the synaptic or extrasynaptic origin of NMDA receptor signals to the nucleus. *Cell*. 2013;152(5):1119–1133.
14. Stanika RI, et al. Coupling diverse routes of calcium entry to mitochondrial dysfunction and glutamate excitotoxicity. *Proc Natl Acad Sci U S A*. 2009;106(24):9854–9859.
15. Papouin T, et al. Synaptic and extrasynaptic NMDA receptors are gated by different endogenous coagonists. *Cell*. 2012;150(3):633–646.
16. Wroge CM, Hogins J, Eisenman L, Mennerick S. Synaptic NMDA receptors mediate hypoxic excitotoxic death. *J Neurosci*. 2012;32(19):6732–6742.
17. Baker DA, Xi Z-X, Shen H, Swanson CJ, Kalivas PW. The origin and neuronal function of in vivo nonsynaptic glutamate. *J Neurosci*. 2002;22(20):9134–9141.
18. Baker DA, Shen H, Kalivas PW. Cystine/glutamate exchange serves as the source for extracellular glutamate: modifications by repeated cocaine administration. *Amino Acids*. 2002; 23(1–3):161–162.
19. Massie A, et al. Dopaminergic neurons of system $x(c)^-$-deficient mice are highly protected against 6-hydroxydopamine-induced toxicity. *FASEB J*. 2011;25(4):1359–1369.
20. De Bundel D, et al. Loss of system xc- does not induce oxidative stress but decreases extracellular glutamate in hippocampus and influences spatial working memory and limbic seizure susceptibility. *J Neurosci*. 2011;31(15):5792–5803.
21. Bannai S, Kitamura E. Transport interaction of L-cystine and L-glutamate in human diploid fibroblasts in culture. *J Biol Chem*. 1980;255(6):2372–2376.
22. Lo M, Wang Y-Z, Gout PW. The x(c)- cystine/glutamate antiporter: a potential target for therapy of cancer and other diseases. *J Cell Physiol*. 2008;215(3):593–602.
23. Conrad M, Sato H. The oxidative stress-inducible cystine/glutamate antiporter, system x (c) (–): cystine supplier and beyond. *Amino Acids*. 2012;42(1):231–246.
24. Gasol E, Jiménez-Vidal M, Chillarón J, Zorzano A, Palacín M. Membrane topology of system xc- light subunit reveals a re-entrant loop with substrate-restricted accessibility. *J Biol Chem*. 2004;279(30):31228–31236.
25. Dringen R. Metabolism and functions of glutathione in brain. *Prog Neurobiol*. 2000; 62(6):649–671.
26. McBean GJ. Cerebral cystine uptake: a tale of two transporters. *Trends Pharmacol Sci*. 2002;23(7):299–302.
27. Sasaki H, et al. Electrophile response element-mediated induction of the cystine/glutamate exchange transporter gene expression. *J Biol Chem*. 2002;277(47):44765–44771.
28. Mysona B, Dun Y, Duplantier J, Ganapathy V, Smith SB. Effects of hyperglycemia and oxidative stress on the glutamate transporters GLAST and system xc- in mouse retinal Müller glial cells. *Cell Tissue Res*. 2009;335(3):477–488.
29. Buckingham SC, et al. Glutamate release by primary brain tumors induces epileptic activity. *Nat Med*. 2011;17(10):1269–1274.
30. Albrecht P, et al. Mechanisms of oxidative glutamate toxicity: the glutamate/cystine antiporter system xc- as a neuroprotective drug target. *CNS Neurol Disord Drug Targets*. 2010;9(3):373–382.
31. Domercq M, et al. System xc- and glutamate transporter inhibition mediates microglial toxicity to oligodendrocytes. *J Immunol*. 2007;178(10):6549–6556.
32. Lewerenz J, Maher P, Methner A. Regulation of xCT expression and system x (c) (-) function in neuronal cells. *Amino Acids*. 2012;42(1):171–179.
33. Jabaudon D, Scanziani M, Gähwiler BH, Gerber U. Acute decrease in net glutamate uptake during energy deprivation. *Proc Natl Acad Sci U S A*. 2000;97(10):5610–5615.
34. Gao J, et al. Coupling between NMDA receptor and acid-sensing ion channel contributes to ischemic neuronal death. *Neuron*. 2005;48(4):635–646.
35. Domercq M, et al. P2X7 receptors mediate ischemic damage to oligodendrocytes. *Glia*. 2010;58(6):730–740.
36. Arbeloa J, Pérez-Samartín A, Gottlieb M, Matute C. P2X7 receptor blockade prevents ATP excitotoxicity in neurons and reduces brain damage after ischemia. *Neurobiol Dis*. 2012; 45(3):954–961.
37. Thompson RJ, Zhou N, MacVicar BA. Ischemia opens neuronal gap junction hemichannels. *Science*. 2006;312(5775):924–927.
38. Gebhardt C, Körner R, Heinemann U. Delayed anoxic depolarizations in hippocampal neurons of mice lacking the excitatory amino acid carrier 1. *J Cereb Blood Flow Metab*. 2002;22(5):569–575.
39. Lossi L, Alasia S, Salio C, Merighi A. Cell death and proliferation in acute slices and organotypic cultures of mammalian CNS. *Prog Neurobiol*. 2009;88(4):221–245.
40. Fujimoto S, Katsuki H, Kume T, Kaneko S, Akaike A. Mechanisms of oxygen glucose deprivation-induced glutamate release from cerebrocortical slice cultures. *Neurosci Res*. 2004;50(2):179–187.
41. Andrade AL, Rossi DJ. Simulated ischaemia induces Ca2+-independent glutamatergic vesicle release through actin filament depolymerization in area CA1 of the hippocampus. *J Physiol*. 2010;588(pt 9):1499–1514.
42. Fleidervish IA, Gebhardt C, Astman N, Gutnick MJ, Heinemann U. Enhanced spontaneous transmitter release is the earliest consequence of neocortical hypoxia that can explain the disruption of normal circuit function. *J Neurosci*. 2001;21(13):4600–4608.
43. Baker DA, et al. Contribution of cystine-glutamate antiporters to the psychotomimetic effects of phencyclidine. *Neuropsychopharmacology*. 2008;33(7):1760–1772.
44. Patel SA, Warren BA, Rhoderick JF, Bridges RJ. Differentiation of substrate and non-substrate inhibitors of transport system xc−: an obligate exchanger of L-glutamate and L-cystine. *Neuropharmacology*. 2004;46(2):273–284.
45. Bridges RJ, Natale NR, Patel SA. System xc- cystine/glutamate antiporter: an update on molecular pharmacology and roles within the CNS. *Br J Pharmacol*. 2012;165(1):20–34.
46. Müller M, Somjen GG. Na(+) dependence and the role of glutamate receptors and Na(+) channels in ion fluxes during hypoxia of rat hippocampal slices. *J Neurophysiol*. 2000;84(4):1869–1880.
47. Doherty AJ, Collingridge GL, Jane DE. Antagonist activity of alpha-substituted 4-carboxyphenylglycine analogues at group I metabotropic glutamate receptors expressed in CHO cells. *Br J Pharmacol*. 1999;126(1):205–210.
48. Melendez R, Vuthiganon J, Kalivas P. Regulation of extracellular glutamate in the prefrontal cortex: focus on the cystine glutamate exchanger and group I metabotropic glutamate receptors. *J Pharmacol*. 2005;314(1):139–147.
49. Chintala S, et al. Slc7a11 gene controls production of pheomelanin pigment and proliferation of cultured cells. *Proc Natl Acad Sci U S A*. 2005;102(31):10964–10969.
50. Warr O, Takahashi M, Attwell D. Modulation of extracellular glutamate concentration in rat brain slices by cystine-glutamate exchange. *J Physiol*. 1999;514 (514):783–793.
51. Tovar KR, Westbrook GL. The incorporation of NMDA receptors with a distinct subunit composition at nascent hippocampal synapses in vitro. *J Neurosci*. 1999;19(10):4180–4188.
52. Petralia RS, et al. Organization of NMDA receptors at extrasynaptic locations. *Neuroscience*.

2010;167(1):68–87.
53. Paoletti P, Bellone C, Zhou Q. NMDA receptor subunit diversity: impact on receptor properties, synaptic plasticity and disease. *Nat Rev Neurosci*. 2013;14(6):383–400.
54. Fischer G, et al. Ro 25-6981, a highly potent and selective blocker of N-methyl-D-aspartate receptors containing the NR2B subunit. Characterization in vitro. *J Pharmacol Exp Ther*. 1997;283(3):1285–1292.
55. Bartlett TE, et al. Differential roles of NR2A and NR2B-containing NMDA receptors in LTP and LTD in the CA1 region of two-week old rat hippocampus. *Neuropharmacology*. 2007;52(1):60–70.
56. Williams K. Ifenprodil discriminates subtypes of the N-methyl-D-aspartate receptor: selectivity and mechanisms at recombinant heteromeric receptors. *Mol Pharmacol*. 1993;44(4):851–859.
57. Edman S, et al. TCN 201 selectively blocks GluN2A-containing NMDARs in a GluN1 co-agonist dependent but non-competitive manner. *Neuropharmacology*. 2012;63(3):441–449.
58. Okamoto S, et al. Balance between synaptic versus extrasynaptic NMDA receptor activity influences inclusions and neurotoxicity of mutant huntingtin. *Nat Med*. 2009;15(12):1407–1413.
59. Xia P, Chen HV, Zhang D, Lipton SA. Memantine preferentially blocks extrasynaptic over synaptic NMDA receptor currents in hippocampal autapses. *J Neurosci*. 2010;30(33):11246–11250.
60. Frizelle PA, Chen PE, Wyllie DJA. Equilibrium constants for (R)-[(S)-1-(4-bromo-phenyl)-ethylamino]-(2,3-dioxo-1,2,3,4-tetrahydroquinoxalin-5-yl)-methyl]-phosphonic acid (NVP-AAM077) acting at recombinant NR1/NR2A and NR1/NR2B N-methyl-D-aspartate receptors: implications for studies of synaptic transmission. *Mol Pharmacol*. 2006;70(3):1022–1032.
61. Abramov AY, Scorziello A, Duchen MR. Three distinct mechanisms generate oxygen free radicals in neurons and contribute to cell death during anoxia and reoxygenation. *J Neurosci*. 2007;27(5):1129–1138.
62. Baek S, et al. Exploratory clinical trial of (4S)-4-(3-[18F]fluoropropyl)-L-glutamate for imaging xC- transporter using positron emission tomography in patients with non-small cell lung or breast cancer. *Clin Cancer Res*. 2012;18(19):5427–5437.
63. Koglin N, et al. Specific PET imaging of xC- transporter activity using a 18F-labeled glutamate derivative reveals a dominant pathway in tumor metabolism. *Clin Cancer Res*. 2011;17(18):6000–6011.
64. Rojas S, et al. Modest MRI signal intensity changes precede delayed cortical necrosis after transient focal ischemia in the rat. *Stroke*. 2006;37(6):1525–1532.
65. Groc L, et al. NMDA receptor surface mobility depends on NR2A-2B subunits. *Proc Natl Acad Sci U S A*. 2006;103(49):18769–18774.
66. Harris AZ, Pettit DL. Extrasynaptic and synaptic NMDA receptors form stable and uniform pools in rat hippocampal slices. *J Physiol*. 2007;584(pt 2):509–519.
67. Hamann M, Rossi DJ, Marie H, Attwell D. Knocking out the glial glutamate transporter GLT-1 reduces glutamate uptake but does not affect hippocampal glutamate dynamics in early simulated ischaemia. *Eur J Neurosci*. 2002;15(2):308–314.
68. Savaskan NE, et al. Small interfering RNA-mediated xCT silencing in gliomas inhibits neurodegeneration and alleviates brain edema. *Nat Med*. 2008;14(6):629–632.
69. Pampliega O, et al. Increased expression of cystine/glutamate antiporter in multiple sclerosis. *J Neuroinflammation*. 2011;8(1):63.
70. Qin Z, et al. Upregulation of xCT by KSHV-encoded microRNAs facilitates KSHV dissemination and persistence in an environment of oxidative stress. *PLoS Pathog*. 2010;6(1):e1000742.
71. Ogunrinu TA, Sontheimer H. Hypoxia increases the dependence of glioma cells on glutathione. *J Biol Chem*. 2010;285(48):37716–37724.
72. Farkas E, Pratt R, Sengpiel F, Obrenovitch TP. Direct, live imaging of cortical spreading depression and anoxic depolarisation using a fluorescent, voltage-sensitive dye. *J Cereb Blood Flow Metab*. 2008;28(2):251–262.
73. Plenz D, Kitai ST. Organotypic cortex-striatum-mesencephalon cultures: the nigrostriatal pathway. *Neurosci Lett*. 1996;209(3):177–180.
74. Cavaliere F, Dinkel K, Reymann K. The subventricular zone releases factors which can be protective in oxygen/glucose deprivation-induced cortical damage: an organotypic study. *Exp Neurol*. 2006;201(1):66–74.
75. Zimmer J, Kristensen BW, Jakobsen B, Noraberg J. Excitatory amino acid neurotoxicity and modulation of glutamate receptor expression in organotypic brain slice cultures. *Amino Acids*. 2000;19(1):7–21.
76. Graulich J, et al. Acute neuronal injury after hypoxia is influenced by the reoxygenation mode in juvenile hippocampal slice cultures. *Brain Res Dev Brain Res*. 2002;137(1):35–42.
77. Ruiz A, Matute C, Alberdi E. Endoplasmic reticulum Ca(2+) release through ryanodine and IP(3) receptors contributes to neuronal excitotoxicity. *Cell Calcium*. 2009;46(4):273–281.
78. Justicia C, Pérez-Asensio FJ, Burguete MC, Salom JB, Planas AM. Administration of transforming growth factor-α reduces infarct volume after transient focal cerebral ischemia in the rat. *J Cereb Blood Flow Metab*. 2001;21(9):1097–1104.